

A Review of Magnetic Cellular Automata Systems

Sanjukta Bhanja and Javier Pulecio

Nano-Computing Research Group, Electrical Engineering Department, University of South Florida

(bhanja@usf.edu, javier.pulecio@gmail.com)

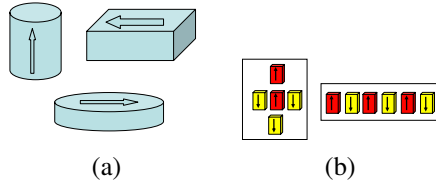


Fig. 1. Magnetic computing basics. (a) Some example nanomagnet shapes. Two dominant ground state directions enumerate logic 1 and 0. (b) A linear arrangement of cells can act as a wire. Majority logic is natural to MCA and is the basic gate for MCA circuits. It has been demonstrated experimentally [10].

Abstract—In this work, we provide a literature review of magnetic cellular automata (MCA) systems. Magnetic Cellular Automata offers promise of low power and room temperature operations. Experimental proof-of-concepts of various logical components are already demonstrated and tested. In architecture, various forms of field induced clocking have been proposed. We direct the authors to most of the achievements and lead them to a few open problems.

I. INTRODUCTION

Field coupled computing is a radically different computing paradigm where electrical, magnetic, or spin coupling among nano-devices are utilized for computation. Cellular automata architecture (one of the architectural theme of the field-coupled computing paradigm) has three/four major breed: Magnetic, Molecular, Atomic and electronic. Cellular automata architectures through Columbic interactions of electrons (Quantum-dot cellular automata, E-QCA) have been proposed, fabricated and analyzed [1], [2], [3], [4]. Note that in spite of ultra-low temperature operation requirements, many works (list above is not complete) all over the world surround this version of QCA using a freeware tool implemented by Walus *et al.* [5].

In molecular cellular automata, the promise of room temperature operation is present and extensive studies on fabrication and architecture [6], [7], [8] have been conducted. Researchers are still working on a stable structure of the molecules and the assembly process. In atomic cellular automata [9], a silicon atom dangling bond (DB) is used as a quantum dot. As individual cells, they work perfectly as room-temperature QCA cell. Neighbor interaction in a cellular automata is an open study.

This work focuses on Magnetic cellular automata (MCA). It possesses all the attractive features of cellular automata, namely wireless system (information transfer through neighbor interaction and not through wires), low power operation. Additionally, MCA systems benefit from vast knowledge/resources from magnetism research (to name a few: modifying remanence and coercivity by shape engineering, resources from high density magnetic storage). Magnetic cellular automata has already been proven to operate at room temperature. In this work, we would enumerate all the significant growths as well as a few unsolved problems/challenges.

II. FUNDAMENTALS

The basic unit of computation is a nanomagnet with dimensions and materials such that it exhibits single domain behavior. Material and geometric shape anisotropy can be exploited to orient the direction of the overall, ground state, least energy magnetization along a desired easy-axis dimension. Fig. 1(a) shows some example nanomagnet shapes with one of their dominant, ground state, magnetization direction. This direction and its opposite, which will also be another ground state, can be used to represent the logic states 0 and 1. Fig. 1(b) shows some example configurations. One of the efforts in nanomagnetic logic [10] has been to build logic gates by mapping the logic onto the ground state configuration.

We can model the single domain behavior of each nanomagnet as a single “Heisenberg spin” vector, with its orientation as a continuous variable. The evolution of the magnetization of any (i -th) nanomagnet can be described by the Landau-Lifshitz-Gilbert equation of magnetic dynamics, containing reactive and dissipative terms.

$$\frac{d\mathbf{M}^{(i)}}{dt} = -\gamma\mathbf{M}^{(i)} \times \mathbf{B}^{(i)} - \frac{\alpha\gamma}{M_s}\mathbf{M}^{(i)} \times (\mathbf{M}^{(i)} \times \mathbf{B}^{(i)}) \quad (1)$$

where (i) $\mathbf{M}^{(i)}$ is the magnetization of the i -th magnet, (ii) γ is a precession coefficient, and (iii) α is the damping factor. The local effective field, $\mathbf{B}^{(i)}$, is given by $-\partial\mathcal{H}^{(i)}/\partial\mathbf{M}^{(i)}$, where $\mathcal{H}^{(i)}$ is the Hamiltonian component of the i -th magnet. The total Hamiltonian of an arrangement of magnets is the sum of these individual Hamiltonians and is given by

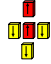



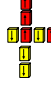



$$\begin{aligned} \mathcal{H} = & \sum_i \mathbf{D}^i \left(\mathbf{M}^{(i)} \right)^T \mathbf{M}^{(i)} + \sum_i \sum_{j \neq i} \left(\mathbf{M}^{(i)} \right)^T \mathbf{C}(i, j) \mathbf{M}^{(j)} \\ & + \sum_i \left(\mathbf{M}^{(i)} \right)^T \mathbf{B}_{ext} \end{aligned} \quad (3)$$

where \mathbf{D}^i is the demagnetization tensor of the i -th magnet, capturing the shape anisotropy, $\mathbf{C}(i, j)$ is the interaction term between the i -th and j -th magnet, \mathbf{B}_{ext} is the external field neglecting crystalline anisotropy as shape anisotropy dominates for elongated pillar magnets [16]. At equilibrium, the value of $\mathbf{M}^{(i)}$, $i = 1, \dots, N$ minimizes the total Hamiltonian. For elongated, pillar, type magnet with shape anisotropy, the magnetic vectors will be along the linear dimension.

III. FABRICATION TECHNIQUES AND EXPERIMENTAL DEMONSTRATION

Most of the experimental demonstrations have followed similar mechanism proposed by [10]. The fabrication process differs between groups accounting for the equipments’ diversity and features. Fabrication is in general accomplished via a standard electron beam lithography process with the Nabyity NPGS

TABLE I
EXPERIMENTAL DEMONSTRATION OF LOGIC COMPONENT,* INDICATES LARGEST CELLS FABRICATED

Logic Component	Shape and minimum Size of Nanomagnets	Schematic	Number of cells	Input	Output Observed
Majority Gate [10]	Rectangular; 135.X70.X30 nm^3		5	Through explicit neighbor magnets	Magnetic Force Microscopy
Ferromagnetic interconnect [11]	Rectangular; 100.X50.X20 nm^3		16	Through explicit neighbor magnets	Magnetic Force Microscopy
Antiferromagnetic interconnect [11]	Rectangular; 100.X50.X20 nm^3		64	Through explicit neighbor magnets	Magnetic Force Microscopy
Fanout [12]	Rectangular; 200.X100.X40 nm^3		16	No input, energy minimum	Magnetic Force Microscopy
Majority with lines [11]	Rectangular; 200.X100.X40 nm^3		9	Through explicit neighbor magnets	Magnetic Force Microscopy
Co-planar Cross-wire [13]	Rectangular; 100.X50.X20 nm^3		10, 120*	No input, energy minimum	Magnetic Force Microscopy
NAND/NOR [14]	Rectangular; 200 X 100.X10 nm^3		5	Field induced	Magnetic Force Microscopy
AND/OR [15]	Rectangular; 150.X60.X40 nm^3		3	Through Explicit neighbor interaction	Magnetic Force Microscopy

system to expose patterns on a Si wafer with a single layer of PMMA resist. A film of desired thickness Permalloy was evaporated using a Electron Beam Evaporator. The patterns are analyzed and characterized by Scanning electron microscopy. Magnetic Force Microscopy is in general used for obtaining qualitative magnetic measurements. Experimental demonstrations have a few common features, namely use of rectangular/elliptic magnets, statically applying inputs to demonstrate various input combinations, qualitative outputs through magnetic force microscopes. In Table I, we tabulate all the logical elements till date, that are fabricated to the best of our knowledge. Evidently, significant progress is made in creating logical elements and building blocks. It is time to focus on architecture to create larger experimental demonstrations.

IV. ARCHITECTURE AND CLOCKING

As noted in [11], [17], in magnetic logic, clocking is extremely crucial in terms of fundamental operation and not just from timing and synchronization point of view. It is shown that even the erroneous state is meta-stable and requires external energy to reach the correct ground state. Various clocking schemes are currently proposed. The first one was an experimental demagnetization scheme with three protocols [17], where Y and Z hard axis fields were separately provided and the samples were also subjected to rotating magnetic field. The observation was that rotating magnetic field was best for the perfect ordering. Another outcome of this study was to find optimal shapes for the nanomagnets.

In Table II, we present the salient works in clocking. Most of

TABLE II
CLOCKING SCHEMES

Schemes	Basic Feature	Feasibility	Validation
Hard Axis clock [18], [19]	Field inducing in hard axis using splitter cell or trapezoidal cell	Orders large array	Simulation based [20]
Hard Axis clock [21]	Field inducing in hard axis taking one cell in one clock zone	Orders large array but hard to implement	Simulation based [20]
MTJ-based Clock [22]	Field inducing by MTJ	Hard to implement .1 nm feature-size	Simulation based [20]
Hard Axis clock [23]	Field inducing in hard axis using bi-axial anisotropy	orders large array; No fabrication results	Simulation based [20]
Hard Axis clock [24]	Field inducing in hard axis	Domino effect in two cells	Magnetic images
Rotating Field [15]	Shown for various shapes	Hard for integration	Magnetic images

the work are based on providing an adiabatic hard axis field and releasing, upon which the computation can be performed.

V. PERFORMANCE PREDICTIONS

Many works are focused on performance predictions in terms of device density, power dissipation and switching speed for MCA. A pioneering effort by Csaba *et al.* [25], where modeling MCA magnetic behavior as a circuit was first proposed. In this work, individual cell's magnetization was modeled as currents in the inductors (inductance reflecting demag factors of the cell). The coupling between nanomagnets were explicitly modeled by C_{ij} capturing the mutual interaction between

neighboring cells.

Device density was estimated to be 10^{10} cells in a square centi-meter considering thermal stability [25]. The switching speed is calculated as a few hundred MHz since adiabatic clocking was assumed for ordering the magnets.

Magnetic cellular automata works as a magnetic amplifier [26]. The power gain relates to the fact that magnets in the direction of information flow injects increasingly larger power towards the receiving end neighbor [26] and power dissipation was predicted in the order of $100 kT$ for individual magnet switching at a switching speed of 1 nano-second. When adiabatic clocking is assumed the power dissipation drops to $10 kT$ at 10^{-7} s for a magnet of dimension $120 \times 60 \times 20 nm^3$.

Researchers have studied multiple large logical networks, namely 32 bit fulladder [18] as well as DCT [22]. In [19], authors have pointed out multiple realistic scenario where power dissipation projection still was order of magnitude better than sub-90 nm CMOS. Current requirements were shown to the order of mA for clocking. In conclusion, in many of these architectures, large ordering lengths are assumed. There is a critical need to experimentally validate clocking schemes.

VI. RELIABILITY AND DEFECTS TOLERANCE

In this section, we would first focus on reliability studies and then concentrate on geometric defects. Reliability study was first conducted with respect to various demagnetizing field in [17]. Authors have shown that rotating magnetic field was best for array ordering. Also half-circular shape was best in term of ordering. Reliability study is also performed for rectangular wires that are both ferro (ferro-wire) and anti-ferromagnetically coupled (AF) in [27]. Results indicate that ferro-wires are more stable and robust towards various demagnetizing clocking field. The authors reported that kink energy was higher for ferro-wires and so they were more prone to ground states than AF wires. A probabilistic model for magnetic wire were studied in [28] where error increased with length. This analysis was based on assuming probability of error and not assuming any masking. Geometric defects were studied for single domain magnetic cell in [29], [30]. The defect masking was presented based on a clock that was not functional for larger array [18]. A need for defect tolerance and defect masking is critical provided ordering of the cells is perfect.

VII. INPUT/OUTPUTS

On-chip input and readout are open area of research in MCA systems. In this section, we first discuss the two existing works on inputs [31], [24]. In [31], experimentally on-chip input was provided to the MCA system consisting of two cells aligned ferromagnetically. A Cu wire with yoke was placed to accomplish current-controlled wire switching. Peak current of 680 mA was reported to accomplish switching of both the magnets. Note that, both the magnets (300 nm apart: no mutual interaction) are influenced by a magnetic field caused by the current and a easy axis to easy axis switching took place. The important aspect of this work is that on-chip wiring was demonstrated for ferro-wires. However, neighbor driving the next neighbor was not evident since the field was global to both the magnets and magnets were far apart. For anti-ferro wires and majority gate however, localized field would be an important issue. In [24], a magnetized AFM tip was scripted to write to individ-

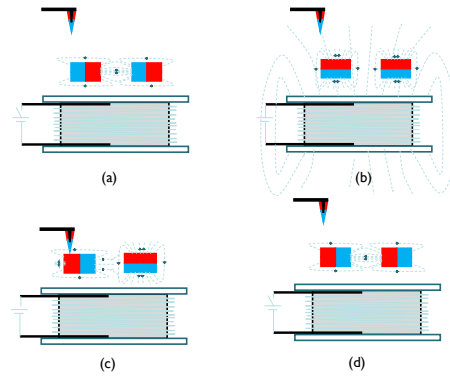


Fig. 2. (I) Input provided through on-chip wire to switch magnets from “1” to “0” easy-easy axis switching (II) Sequence of experiments to demonstrate localized input, need for hard axis field and intended neighbor interact under the influence of the hard axis field.

ual magnet and state of the magnet were changed through field-induced switching (see Fig. 2. However, neighboring magnets did not get influenced. A hard axis field is then created by an in-situ electromagnet. Two important observations were confirmed: (a) switching field required to switch the driver magnet reduced significantly (from 8.5 mTesla to 2.5 mTesla) with the hard-axis field and (b) neighbor interaction was evident under the influence of the hard-axis field of 45 mTesla.

For read-out, one could rely on resistance change in a magnetic wire which is created by trapping of domain wall by the output nanomagnets [32]. On-chip localized reading and writing is an open area of research in MCA systems. One would envision a possible fusion of MRAM and MCA however, the filed driven clocking is going to need significant transformation so that read-out and writing is protected from errors.

VIII. NON-BOOLEAN LOGIC

Most the MCA design and synthesis has been focusing on Boolean Logic. In this section, we will briefly point the reader to a Non-Boolean local synthesis [33] that uses the magnetic interaction to solve quadratic energy minimization problem. In this work, a mid-level computer vision problem of grouping is targeted. In Fig. 3a, an aerial image of buildings is shown. Fig. 3b is the result of an edge-detection algorithm that identifies salient edges of the building. The problem of grouping relates to identifying the edges that can be grouped as part of one object. Grouping is followed by library matching to solve pattern recognition problem. Initial proof-of-concept in [33], [34] shows that edges can be mapped to individual single domain magnets and their relative placements can be arrived statistically based on the saliency and affinity of the edges. One can solve the grouping by measuring the change of magnetization due to neighbor interaction. Experimental validation, programmable architecture for non-Boolean computing remains an open problem.

IX. CONCLUSION

As discussed in the previous sections, tremendous growth and accomplishments have been achieved in this research direction. The challenges lie mostly in input, output and hybrid integration of these devices. Some of the open problems are (a) how to provide local control in terms of input, output and clocking?

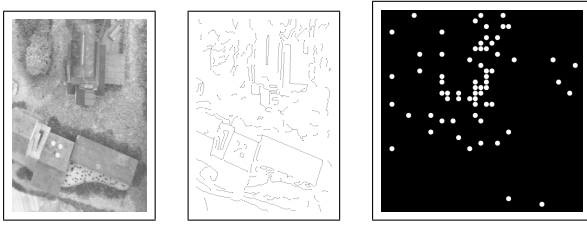


Fig. 3. (a) Aerial image of buildings. (b) Edges (or boundary features) detected in the image. Which of these are from the building? (c) Synthesis of the MCA layout that help find the important edges in (b).

(b) Would we be able to leverage from magnetic memory technology effectively? (c) Can non-Boolean problem mapping be more computationally attractive? Room temperature low power robust operations are an asset to this technology along with relative ease of fabrication. Many logical components are already demonstrated and tested. In [19], authors have reported that energy-delay-product of various latest CMOS technologies are few hundreds of order of magnitude greater than that of MCA for various field-induced clocking schemes for systolic MCA logic. In [22], a DCT implementation using MCA with steel solenoid core yielded orders of magnitudes lower dissipated power compared to 45 nm CMOS technology while keeping the frequency constant. However, further study is necessary to calibrate these claims with realistic back-end circuit design and integration issues. As a consequence of these promises and potentials, ITRS roadmap [35] has shown magnetic logic as one of target emerging devices and architecture in 2009 and we hope that in the coming decade, many of the integration issues would be resolved.

Acknowledgements: Authors would like to acknowledge partial support from NSF CAREER grant 0639624, NSF EMT grant 0829838.

REFERENCES

- [1] C. Lent and P. Tougaw, "A device architecture for computing with quantum dots," in *Proceeding of the IEEE*, vol. 85-4, pp. 541–557, April 1997.
- [2] A. Orlov, R. Kummamuru, R. Ramasubramaniam, C. Lent, G. Bernstein, and G. Snider, "Clocked quantum-dot cellular automata shift register," *Surface Science*, vol. 532, pp. 1193–1198, 2003.
- [3] M. Niemier and P. M. Kogge, "The "4-diamond circuit" a minimally complex nano-scale computational building block in qca," in *IEEE Computer Society Annual Symposium on VLSI Emerging Trends in VLSI Systems Design*, pp. 3–10, Feb 2004.
- [4] V. Vankamamidi, M. Ottavi, and F. Lombardi, "A line-based parallel memory for QCA implementation," *IEEE Transactions on Nanotechnology*, vol. 4, pp. 690–698, Nov. 2005.
- [5] K. Walus, T. Dysart, G. Jullien, and R. Budiman, "QCADesigner: A rapid design and simulation tool for quantum-dot cellular automata," *IEEE Trans. on Nanotechnology*, vol. 3, pp. 26–29, March 2004.
- [6] Q. Hang, Y. Wang, M. Lieberman, and G. Bernstein, "Molecular patterning through high-resolution polymethylmethacrylate masks," *Applied Physics Letters*, vol. 80, pp. 4220–4222, June 2002.
- [7] W. Hu, K. Sarveswaran, M. Lieberman, and G. H. Bernstein, "High-resolution electron beam lithography and DNA nano-patterning for molecular QCA," *IEEE Transactions on Nanotechnology*, vol. 4, pp. 312–316, May 2005.
- [8] T. Dysart and P. Kogge, "Probabilistic analysis of a molecular quantum-dot cellular automata adder," 2007.
- [9] M. B. Haider, J. L. Pitters, G. A. DiLabio, L. Livadaru, J. Y. Mutus, and R. A. Wolkow, "Controlled coupling and occupation of silicon atomic quantum dots at room temperature," *Phys. Rev. Lett.*, vol. 102, p. 046805, Jan 2009.
- [10] A. Imre, G. Csaba, L. Ji, A. Orlov, G. Bernstein, and W. Porod, "Majority Logic Gate for Magnetic Quantum-Dot Cellular Automata," 2006.
- [11] A. Orlov, A. Imre, G. Csaba, L. Ji, W. Porod, and G. Bernstein, "Magnetic Quantum-Dot Cellular Automata: Recent Developments and Prospects," *Journal of Nanoelectronics and Optoelectronics*, vol. 3, no. 1, pp. 55–68, 2008.
- [12] E. Varga, S. Liu, M. Niemier, W. Porod, X. Hu, G. Bernstein, and A. Orlov, "Experimental demonstration of fanout for nanomagnet logic," in *Device Research Conference (DRC), 2010*, pp. 95–96, IEEE, 2010.
- [13] J. Pulecio and S. Bhanja, "Magnetic Cellular Automata Coplanar Cross Wire Systems," *Journal of applied physics*, 2010.
- [14] R. Nakatani, H. Nomura, and Y. Endo, "Magnetic logic devices composed of permalloy dots," in *Journal of Physics: Conference Series*, vol. 165, p. 012030, IOP Publishing, 2009.
- [15] M. Niemier, E. Varga, G. Bernstein, W. Porod, M. Alam, A. Dingler, A. Orlov, and X. Hu, "Boolean logic through shape-engineered magnetic dots with slanted edges," *IEEE Trans. on Nanotechnology*, 2010.
- [16] J. Deutsch, T. Mai, and O. Narayan, "Hysteresis multicycles in nanomagnet arrays," *Physical Review E*, vol. 71, no. 2, p. 26120, 2005.
- [17] G. Bernstein, A. Imre, V. Metlushko, A. Orlov, L. Zhou, L. Ji, G. Csaba, and W. Porod, "Magnetic QCA systems," *Microelectronics Journal*, vol. 36, no. 7, pp. 619–624, 2005.
- [18] M. Niemier, M. Alam, X. Hu, G. Bernstein, W. Porod, M. Putney, and J. DeAngelis, "Clocking structures and power analysis for nanomagnet-based logic devices," in *Proceedings of the 2007 international symposium on Low power electronics and design*, pp. 26–31, ACM New York, NY, USA, 2007.
- [19] M. Crocker, X. Hu, and M. Niemier, "Design and comparison of NML systolic architectures," in *Proceedings of the 2010 IEEE/ACM International Symposium on Nanoscale Architectures*, pp. 29–34, IEEE Press, 2010.
- [20] M. Donahue and D. Porter, "OOMMF User's guide," *National Institute of Standards and Technology, Gaithersburg, MD*, 1999.
- [21] A. Kumari and S. Bhanja, "Landauer clocking for magnetic cellular automata (mca) arrays," *Very Large Scale Integration (VLSI) Systems, IEEE Transactions on*, 2009.
- [22] C. Augustine, B. Behin-Aein, X. Fong, and K. Roy, "A design methodology and device/circuit/architecture compatible simulation framework for low-power magnetic quantum cellular automata systems," in *Proceedings of the 2009 Asia and South Pacific Design Automation Conference*, pp. 847–852, IEEE Press, 2009.
- [23] D. Carlton, N. Emlay, E. Tuchfeld, and J. Bokor, "Simulation Studies of Nanomagnet-Based Logic Architecture," *Nano Letters*, vol. 8, no. 12, pp. 4173–4178, 2008.
- [24] D. Karunaratne, J. Pulecio, and S. Bhanja, "Driving magnetic cells for information storage and propagation," in *Nanotechnology Materials and Devices Conference (NMDC), 2010 IEEE*, pp. 360–363, IEEE.
- [25] G. Csaba, A. Imre, G. Bernstein, W. Porod, and V. Metlushko, "Nanocomputing by field-coupled nanomagnets," *IEEE Transactions on Nanotechnology*, vol. 1, no. 4, pp. 209–213, 2002.
- [26] G. Csaba, P. Lugli, A. Csurgay, and W. Porod, "Simulation of power gain and dissipation in field-coupled nanomagnets," *Journal of Computational Electronics*, vol. 4, no. 1, pp. 105–110, 2005.
- [27] J. Pulecio, P. Pendru, A. Kumari, and S. Bhanja, "Magnetic cellular automata wire architectures," *IEEE Transactions on Nanotechnology*, 2011. Accepted.
- [28] T. Dysart and P. Kogge, "Analyzing the inherent reliability of moderately sized magnetic and electrostatic QCA circuits via probabilistic transfer matrices," *Very Large Scale Integration (VLSI) Systems, IEEE Transactions on*, vol. 17, no. 4, pp. 507–516, 2009.
- [29] M. Niemier, M. Crocker, and X. S. Hu, "Fabrication variations and defect tolerance for nanomagnet-based qca," pp. 534–542, 2008.
- [30] A. Kumari, J. F. Pulecio, and S. Bhanja, "Defect characterization in magnetic field coupled arrays," in *IEEE Symposium on Quality of Electronic Design*, pp. 436–441, 2009.
- [31] M. Alam, M. Siddiq, G. Bernstein, M. Niemier, W. Porod, and X. Hu, "On-chip clocking for nanomagnet logic devices," *Nanotechnology, IEEE Transactions on*, vol. 9, no. 3, pp. 348–351, 2010.
- [32] L. Ji, A. Orlov, G. Bernstein, W. Porod, and G. Csaba, "Domain-wall trapping and control on submicron magnetic wire by localized field," in *Nanotechnology, 2009. IEEE-NANO 2009. 9th IEEE Conference on*, pp. 758–762, IEEE, 2010.
- [33] S. Sarkar and S. Bhanja, "Direct Quadratic Minimization Using Magnetic Field-Based Computing," in *Design and Test of Nano Devices, Circuits and Systems, 2008 IEEE International Workshop on*, pp. 31–34, IEEE, 2008.
- [34] A. Kumari, S. Sarkar, J. Pulecio, D. Karunaratne, and S. Bhanja, "Study of Magnetization State Transition in Closely Spaced Nanomagnet 2D array for computation," *Journal of Applied Physics*, 2011. Accepted.
- [35] "International technology roadmap for semiconductor," 2009.